Rain Attenuation Characteristics of Ku-band Satellite Signals in relation to the Wind Velocities observed on the Ground

Yutaka Inamori [1], Yoshiaki Shibagaki [1], Yasuyuki Maekawa [1]
[1] Department of Telecommunications & Computer Network, Osaka Electro-Commun. Univ.,
18-8 Hatsucho, Neyagawa, Osaka 572-8530, Japan, "mf12a001@oecu.jp"

1. Introduction

The recent satellite communications tend to use high frequency bands of more than 10 GHz, in addition to the traditional C band of 6/4 GHz. In these higher frequency bands, however, the rain attenuation of radio waves becomes one of the severe problems of satellite communications. Thus, detailed observations and statistical analyses of rain attenuation characteristics are necessary for reliable operations of satellite communication links [1]. In this study, Ku-band satellite signal levels have been simultaneously observed at Osaka Electro-Communication University (OECU, Neyagawa, Osaka), the Research Institute for Sustainable Humanosphere (Uji, Kyoto) and the Shigaraki MU radar observatory (Koga, Shiga) of Kyoto University since September 2002 [2]. The direction and speed of rain area motions are estimated from the time differences in the attenuation detected at these three locations, and compared with the wind direction and speed measured by the AMeDAS located at a nearby station (Hirakata, Osaka) on the ground.

2. Measurement Systems

At the three stations, the Ku-band broadcasting satellite (BS) signals (11.8GHz, RHCP, EL=41 deg) have been continuously observed. At RISH in Uji, however, the Ku-band down-link signal (12.7GHz, HP, EL=49 deg) of Superbird C that connects RISH to the Equatorial Atmosphere Radar (EAR) had been observed instead of the BS signal up to July 2005. These signal levels are recorded by personal computers equipped with 16 bit AD converters. For the estimation of attenuation and its statistics, the observed data are further averaged over 1 min. RISH in Uji, Kyoto is located 23.3 km northwest (16.0 km, 16.9 km) from OECU in Neyagawa, Osaka, while MU in Koga, Shiga is located 45.9 km east northeast (44.2 km, 12.4 km) from OECU. The geographical relationship among the three locations is shown in Fig.1.

To infer the direction and speed of rain area motion over these three locations, the time series of rain attenuation measured at each station are compared at 1 min interval in every rainfall event. The time difference of attenuation occurrence is estimated from the peak of the cross-correlation function calculated between each combination of the two among the three locations. These rain area motions inferred from the time difference of the attenuation occurrence are proved to agree well with those of the passage direction and speed perpendicular to the rain fronts on weather charts published by Japan Meteorological Agency at three or 12 hour intervals [2]. Also, these rain area motions, as a whole, agree with wind direction and speed actually measured by the MU radar (Koga, Shiga) in the upper air at 2-6 km height [3].

AMeDAS (Automated Meteorological Data Acquisition System) is a high-resolution surface observation network developed by Japan Meteorological Agency, being primarily used for gathering regional weather data and verifying forecast performance all over Japan. It started operation in November 1974, and now consists of about 1300 stations with automatic observation equipment for such as rainfall rate, air temperature, wind direction and speed. These stations are located at an average interval of 17 km throughout Japan, and the automatic observations are basically conducted at 10 min intervals. In this study, we use the wind direction and speed data that has been observed by the AMeDAS located in Hirakata city 6.7 km north-east from our university (OECU). The data are published in the web site at one hour interval, and we averaged these values for 2-6 hours according to the duration time of each rainfall event.

3. Observational Results

Figure 2 shows an example of rain attenuation observed at the three locations on June 29, 2010. In Fig. 2(a), we can see that the attenuation of 11 dB occurred during 1:00-4:00 LT at each location in order of OECU (blue line), RISH (green line), and MU (red line). In Fig. 2(b), cross-correlation functions of the rain attenuation are then calculated between OECU and the other locations. The red line indicates the result obtained from the combination of OECU and MU, while the green line is that of OECU and RISH, for the lag times from -60 to 60 min. The correlation values of nearly 0.9 are found in the peaks of both cross-correlation functions. The lag times obtained from these peaks indicates that the attenuation, on an average, occurred 19 min later (+19 min) at RISH and 56 min later (+56 min) at MU, respectively, than at OECU. Also, the high correlation values of about 0.9 suggest that the three locations should similarly observe the attenuation caused by rain bands or rain cells of the same rain front passing over them.

Fig.2(c) thus shows speed and direction (arrow) of the rain area estimated from the time differences in attenuation occurrence among the three locations, as well as their geographical relationship with OECU. Green and red dashed lines indicate the positions of the rain front inferred at RISH and MU, respectively, which passed over them in this order. The rain area associated with the front is shown to move eastward at a speed of 12.82 m/s. The direction of the motion is 94.4 degree clockwise from the north.

Next, Table 1 summarizes the rain area motions inferred from these three-location BS radio wave measurements and the ground wind velocities simultaneously obtained from AMeDAS at the Hirakata station 6.7 km north-east from OECU during one year of 2010. We obtained eight samples of both rain area motion and ground velocity in this year, and the relationship between their directions and speeds are depicted in Fig.3. It is found from Fig.3 that the speeds of the rain area motions in the upper area are, as a whole, several times larger than the wind speeds measured by AMeDAS on the ground. The directions of the rain area motions are, on the other hand, shown to be slightly turned to eastward compared to the ground wind directions.

Finally, Fig.4 indicates scatter plots of (a) directions and (b) speeds between the rain area motions and the ground wind velocities listed in Table 1. Although the number of examples is limited to only eight rainfall events in this year, we can still find considerable correlations between both of them: the correlation coefficients are 0.57 in the directions and 0.51 in the speeds, respectively. So, there still remain possibilities that we may estimate rain area motions in the upper air from ground wind velocities which can be easily obtained from usual routine meteorological measurements, such as AMeDAS. Especially, the direction of rain area motions as regards the alignment of two sites for space diversity was shown to be very important by our previous study [2]. Therefore, the methods to infer the rain area motion in the upper air from the ground wind velocities may have a large impact on the effects of the site diversity techniques for rain attenuation mitigation.

4. Conclusions

The direction and speed of rain area motions are estimated from the time differences in the Ku-band satellite signal attenuation detected at the three locations of Osaka Electro-Communication University (OECU, Neyagawa, Osaka), the Research Institute for Sustainable Humanosphere (Uji, Kyoto), and the Shigaraki MU radar observatory (Koga, Shiga) of Kyoto University. The direction and speed of the rain areas are compared with those of the ground wind velocities observed by AMeDAS at the nearby station 6.7 km north-east from OECU during the year of 2010. Although the simultaneous observations have only eight examples in this year, considerable correlations are found between the rain area motions and the ground wind velocities, suggesting that the direction and speed of the rain areas which is important to site diversity techniques may be easily estimated from the ground wind velocity measurements such as AMeDAS. In the future, further observations of rain area motions and ground wind velocities are needed, and comparison of their directions and speeds should be made with much more examples of longer observational years. Also, direct measurements of upper air motions using the MU radar and other wind profiler networks around the three observational locations are highly desired, to investigate the relationship between rain area motions and wind velocities from the ground to rain height in more detail.

Acknowledgments

The authors deeply thank the staff of the Shigaraki MU radar observatory who assists the measurements in this study.

References

[1] T. Iida, "Satellite communication (in Japanese)," Ohmusha, 1997.

[2] Y. Maekawa, T. Nakatani, Y.Shibagaki, T. Hatsuda, "A Study on Site Diversity Techniques related to Rain Area Motion using Ku-Band Satellite Signals," *IEICE Trans. Commun*. Vol.E91-B, No.6, pp.1812-1818, Jun. 2008.

[3] M. Noyama, Y. Shibagaki, and Y. Maekawa "Rain Attenuation Characteristics of Ku-band Satellite Signals related to Radar Observation of the Wind Velocities at Rain Height," *The 29th AIAA International Communications Satellite Systems Conference* (*ICSSC-2011*), ICSSC-17-2, Nara, Japan, 2011

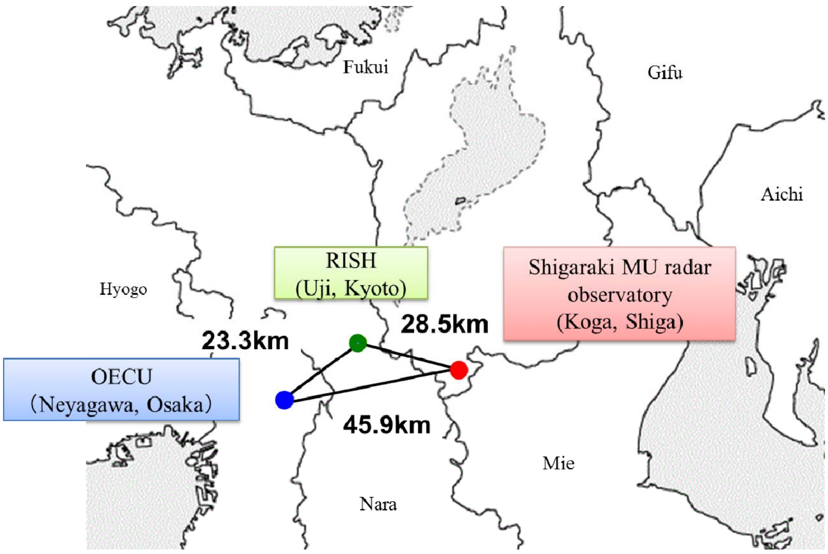

Figure1: Geographical relationship among three observational locations of OECU, RISH, and MU.

(a) (b) (c)

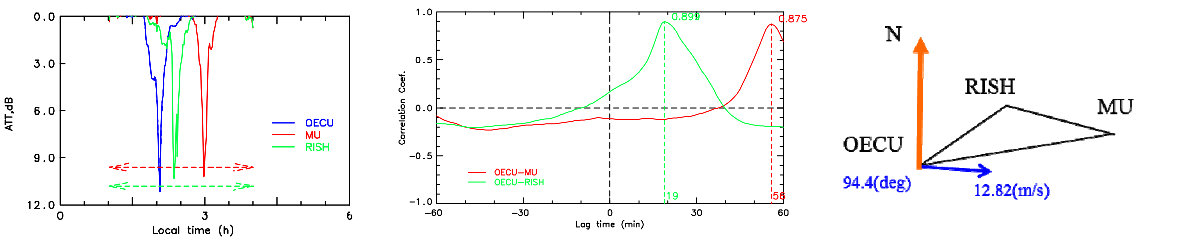

Figure 2: Examples of (a) rain attenuation, (b) cross-correlation functions, (c) direction and speed of rain area motions estimated from the three observational locations on June 29, 2010.

Table 1: Rain area motions inferred from three-location BS measurements and ground wind velocities simultaneously obtained from AMEDAS in 2010

		Rain area motions		Ground wind velocities	
No.	Date	direction [deg]	speed [m/s]	direction [deg]	speed [m/s]
1	Jan. 21	133.3	8.76	176.7	0.7
2	Jan. 28	93.5	22.56	133.3	2.9
3	Mar. 15	114.8	17.64	230.0	3.2
4	May 20	149.7	8.41	230.0	2.3
5	Jun. 29	94.4	12.82	60.0	1.3
6	Jul. 14	78.3	15.89	45.0	1.3
7	Sep. 27	74.6	25.48	188.3	2.4
8	Oct. 3	99.0	12.87	203.0	2.6

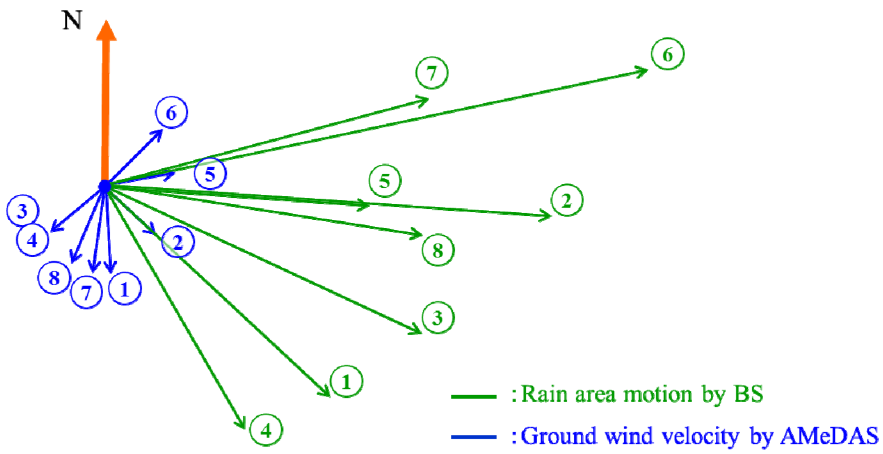

Figure 3: Vector plots of the rain area motions and the ground wind velocities listed in Table 1.

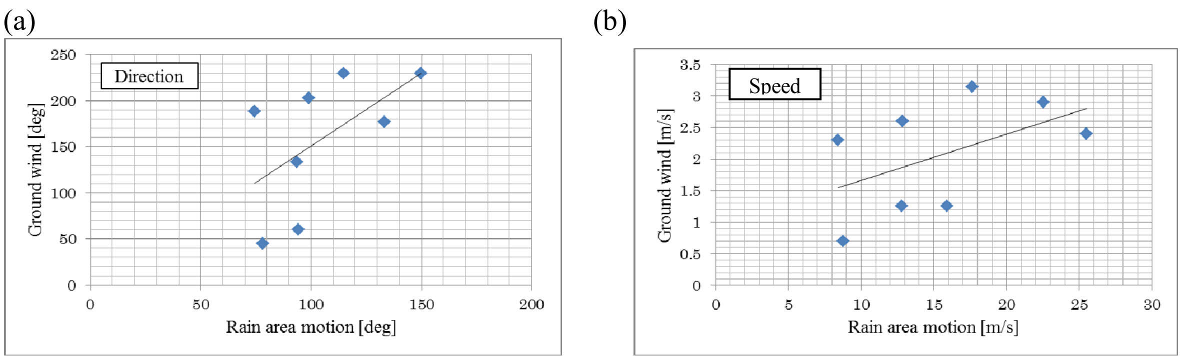

Figure 4: Scatter plots of (a) directions and (b) speeds between the rain area motions and the ground wind velocities.